doi:10.1093/brain/awr283 Brain 2012: 135; 88–104 | 88

BRAIN
A JOURNAL OF NEUROLOGY

Colony-stimulating factor-1 mediates macrophage-related neural damage in a model for Charcot–Marie–Tooth disease type 1X

Janos Groh,[1] Joachim Weis,[2] Hanna Zieger,[1] E. Richard Stanley,[3] Heike Heuer[4] and Rudolf Martini[1]

1 Department of Neurology, Section of Developmental Neurobiology, University of Würzburg, Josef-Schneiderstr. 11, 97080 Würzburg, Germany
2 Institute of Neuropathology, Medical Faculty, RWTH Aachen University, Pauwelsstraße 30, 52074 Aachen, Germany
3 Department of Developmental and Molecular Biology, Albert Einstein College of Medicine, 1300 Morris Park Avenue, Bronx, New York, NY 10461, USA
4 Neuroendocrinology Group, Leibniz Institute for Age Research, Fritz Lipmann Institute, Jena, Germany

Correspondence to: R. Martini
Department of Neurology,
Section of Developmental Neurobiology,
University of Würzburg,
Josef-Schneiderstr. 11,
97080 Würzburg, Germany
E-mail: rudolf.martini@uni-wuerzburg.de

Previous studies in our laboratory have shown that in models for three distinct forms of the inherited and incurable nerve disorder, Charcot–Marie–Tooth neuropathy, low-grade inflammation implicating phagocytosing macrophages mediates demyelination and perturbation of axons. In the present study, we focus on colony-stimulating factor-1, a cytokine implicated in macrophage differentiation, activation and proliferation and fostering neural damage in a model for Charcot–Marie–Tooth neuropathy 1B. By crossbreeding a model for the X-linked form of Charcot–Marie–Tooth neuropathy with osteopetrotic mice, a spontaneous null mutant for colony-stimulating factor-1, we demonstrate a robust and persistent amelioration of demyelination and axon perturbation. Furthermore, functionally important domains of the peripheral nervous system, such as juxtaparanodes and presynaptic terminals, were preserved in the absence of colony-stimulating factor-1-dependent macrophage activation. As opposed to other Schwann cell-derived cytokines, colony-stimulating factor-1 is expressed by endoneurial fibroblasts, as revealed by *in situ* hybridization, immunocytochemistry and detection of β-galactosidase expression driven by the colony-stimulating factor-1 promoter. By both light and electron microscopic studies, we detected extended cell–cell contacts between the colony-stimulating factor-1-expressing fibroblasts and endoneurial macrophages as a putative prerequisite for the effective and constant activation of macrophages by fibroblasts in the chronically diseased nerve. Interestingly, in human biopsies from patients with Charcot–Marie–Tooth type 1, we also found frequent cell–cell contacts between macrophages and endoneurial fibroblasts and identified the latter as main source for colony-stimulating factor-1. Therefore, our study provides strong evidence for a similarly pathogenic role of colony-stimulating factor-1 in genetically mediated demyelination in mice and Charcot–Marie–Tooth type 1 disease in humans. Thus, colony-stimulating factor-1 or its cognate receptor are promising target molecules for treating the detrimental, low-grade inflammation of several inherited neuropathies in humans.

Keywords: inflammation; endoneurial fibroblasts; myelin, axonopathy; neuromuscular junction

Abbreviations: CSF-1 = colony-stimulating factor-1; PMP22 = peripheral myelin protein 22

Received June 6, 2011. Revised August 19, 2011. Accepted August 26, 2011. Advance Access publication November 16, 2011
© The Author (2011). Published by Oxford University Press on behalf of the Guarantors of Brain. All rights reserved.
For Permissions, please email: journals.permissions@oup.com

Introduction

Inherited demyelinating neuropathies of the Charcot–Marie–Tooth type are disabling disorders of the PNS. The genetic causes have been deciphered for many forms (Niemann *et al*., 2006; Scherer and Wrabetz, 2008; Reilly *et al*., 2011) and some pathomechanistic aspects have even been investigated in detail (Pennuto *et al*., 2008; D'Antonio *et al*., 2009); still, these disorders are untreatable (Schenone *et al*., 2011). Of note, studies in animal models for Charcot–Marie–Tooth type 1A previously revealed some promising observations from the systemic application of ascorbic acid as possible treatment approach, but clinical trials so far have failed to provide evidence for the use of this vitamin as a treatment option (Burns *et al*., 2009; Micallef *et al*., 2009; Pareyson and Solari, 2009; Pareyson *et al*., 2011; Schenone *et al*., 2011). Antiprogesterone-based therapies in a rat model is theoretically another option for treating solely Charcot–Marie–Tooth type 1A, but expected serious side effects might prohibit direct clinical application (Meyer zu Horste *et al*., 2007). Thus, at present, only symptomatic and rehabilitative strategies are available to reduce the disabling clinical features (Schenone *et al*., 2011).

We have recently documented that in mouse models for Charcot–Marie–Tooth types 1A, 1B and 1X, low-grade inflammation implicating phagocytosing macrophages substantially contributes to the demyelinating and axonopathic phenotype of the disorders, which might open common therapeutic options for several inherited neuropathies (Ip *et al*., 2006*b*; Fischer *et al*., 2008*a*, *b*; Martini *et al*., 2008; Groh *et al*., 2010; Kohl *et al*., 2010). An important, Schwann cell-borne mediator of the respective detrimental macrophage function is the chemokine CCL2, which is expressed downstream of intracellular activation of the mitogen activated protein (MAP) kinases, extracellular signal-regulated kinase (ERK), and MAP kinase/ERK kinase (MEK) (Fischer *et al*., 2008*a*, *b*; Groh *et al*., 2010; Kohl *et al*., 2010). Another important macrophage activator that has been identified in Charcot–Marie–Tooth type 1B mice is colony-stimulating factor-1 (CSF-1; Carenini *et al*., 2001; Muller *et al*., 2007). As opposed to CCL2, neither the cellular source nor the role of CSF-1 in other Charcot–Marie–Tooth models has been identified. In the present study, we show that CSF-1 is a pivotal macrophage activator in a model for Charcot–Marie–Tooth type 1X and is expressed by endoneurial fibroblasts that form extended cell–cell contacts with endoneurial macrophages. Importantly, we detected similar interactions between CSF-1-producing fibroblasts and macrophages in other Charcot–Marie–Tooth models and in nerve biopsies of human patients with Charcot–Marie–Tooth type 1. Our study shows that CSF-1 is an essential, pathogenic molecule in at least two distinct models for Charcot–Marie–Tooth type 1 and might play a similar role in human Charcot–Marie–Tooth type 1. CSF-1 is therefore another promising target for treating the detrimental, low-grade inflammation of inherited neuropathies.

Materials and methods

Animals

Connexin 32-deficient (Cx32def) mice (Nelles *et al*., 1996) were cross-bred with CSF-1-deficient osteopetrotic (op) mice (Yoshida *et al*., 1990) according to previously published protocols (Kobsar *et al*., 2003; Groh *et al*., 2010). Cx32def mice were on a mixed C57BL/6 × 129Sv genetic background, whereas osteopetrotic mutants were on a uniform C57BL/6 background. In parallel, Cx32def mice were back-crossed for more than six generations to a uniform C57BL/6 background with the typical neuropathological alterations and similar severity of neuropathy as seen in the Cx32def mice of the mixed background. Transgenic (tg) peripheral myelin protein 22-overexpressing mice (PMP22tg) of the C61 strain (Huxley *et al*., 1998) were maintained on the C57BL/6 background. Determination of genotypes was achieved with conventional polymerase chain reaction using isolated DNA from tail biopsies following previously published protocols (Carenini *et al*., 2001; Kobsar *et al*., 2003; Kohl *et al*., 2010). Homozygous osteopetrotic mice presented with all described phenotypic characteristics, including reduced lifespan and body size, precluding comparisons to mice with a wild-type CSF-1 genotype regarding electrophysiological and behavioural analyses. Mice were kept in the animal facility of the Department of Neurology under barrier conditions and all animal experiments were approved by the Regierung von Unterfranken.

Semi-quantitative real-time polymerase chain reaction

Mice were transcardially perfused with phosphate-buffered saline containing heparin and peripheral nerves were quickly dissected, snap frozen in liquid nitrogen and homogenized (ART-MICCRA D-8, ART Labortechnik) in TRIzol® reagent (Invitrogen). Total RNA was isolated according to the guidelines of manufacturers. Concentration and quality of RNA was determined using a BioPhotometer (Eppendorf) and 1 μg of RNA was reverse transcribed in a 100 μl reaction using random hexamer primers (Applied Biosystems). Complementary DNA samples were subsequently analysed as triplicates by semi-quanitiative real-time polymerase chain reaction using pre-developed TaqMan® assays (Murine M-CSF, Mm00432688_m1; eukaryotic 18S ribosomal RNA Endogenous Control, 4319413E) and TaqMan® universal PCR master mix (Applied Biosystems) according to the guidelines of manufacturers and previously published protocols (Fischer *et al*., 2008*a*).

Combined immunohistochemistry and *in situ* hybridization

For the cellular localization of CSF-1 expression, radioactive *in situ* hybridization (CSF-1 messenger RNA) and immunohistochemistry (cell markers) were combined. Fresh frozen femoral quadriceps nerves were cut into 10 μm cross-sections and stored at −80°C until required. After post-fixation in ice-cold acetone or 4% paraformaldehyde in phosphate-buffered saline for 10 min, sections were blocked with 5% bovine serum albumin and 1% normal goat serum in phosphate-buffered saline and incubated with rat anti-mouse CD34 (1:1000, eBioscience; for identifying fibroblasts), rat anti-mouse F4/80 (1:300, Serotec; for identifying macrophages) or rabbit anti-mouse S100β (1:1000, Dako; for identifying Schwann cells) antibodies. Primary antibodies were detected by biotinylated goat anti-rat or goat anti-rabbit IgG (Vector Laboratories) and streptavidin–biotin–peroxidase (Vector Laboratories) complex using diaminobenzidine–HCl and H_2O_2. To prevent RNA degradation, all incubation steps were carried out in the presence of 10 U/ml RNase inhibitor (Ambion). After the peroxidase staining reaction, the *Csf1* transcripts were then localized by *in situ* hybridization using an antisense *Csf1* specific riboprobe and a corresponding sense riboprobe as negative control

(Hristova *et al*., 2010). For microscopic analysis, sections were dipped in Kodak NTB2 nuclear emulsion and stored at 4°C for up to 20 weeks. Autoradiograms were developed, and viewed under dark- and bright-field illuminations using an Olympus AX microscope to detect CSF-1-related silver grains in association with distinct cell types.

Immunohistochemistry

CSF-1 protein and its receptor (CSF-1R) were localized in peripheral nerves that had been loosely teased and spread on glass slides so that nerve fibres and the other endoneurial components were preserved and exposed. Specificity of the antibodies (rabbit anti-mouse CSF-1, 1:300; rabbit anti-mouse CSF-1R, 1:100; Santa Cruz) was controlled by omission of the primary antibodies or use of teased nerve preparations from Cx32def/CSF-1op mice. Briefly, mice were deeply anaesthetized and transcardially perfused with 2% paraformaldehyde in phosphate-buffered saline for 15 min. Femoral quadriceps and sciatic nerves were excised, the perineurium was stripped off, and nerve fibres were loosely separated (teased), air dried and fixed in ice-cold acetone (10 min). Teased nerves were then blocked with 5% bovine serum albumin in phosphate-buffered saline and incubated with primary antibodies overnight at 4°C. To visualize the primary antibodies, teased nerves were incubated with Cy3-conjugated goat anti-rabbit IgG secondary antibodies (Vector Laboratories) for 1 h and nuclei were stained with 4′,6-diamidino-2-phenylindole (DAPI; Sigma-Aldrich).

Quantification of CSF-1-positive fibroblasts or CSF-1-positive macrophages was performed on teased nerves by double labelling of CSF-1 as described in combination with rat anti-mouse CD34 (for fibroblasts; 1:1000, eBioscience) or rat anti-mouse F4/80 (for macrophages; 1:300, Serotec) primary antibodies, and Cy2-conjugated goat anti-rat IgG secondary antibodies (Vector Laboratories). At least 60 fibroblasts or macrophages from three different animals per genotype group were counted and the percentage of CSF-1 immunopositive cells was determined. Double labelling of CSF-1R and F4/80 was achieved accordingly.

Quantification of endoneurial macrophages was performed on 10 μm cross-sections of fresh frozen femoral quadriceps nerves according to previously published protocols (Carenini *et al*., 2001). Endoneurial macrophages were detected using rat anti-mouse F4/80 primary antibodies and Cy3-conjugated goat anti-rat IgG secondary antibodies and nuclei were stained with DAPI (Sigma-Aldrich).

For quantification of macrophages in contact with endoneurial fibroblasts, 10 μm cross-sections of fresh frozen quadriceps nerves were fixed in ice-cold acetone (10 min), blocked with 5% bovine serum albumin in phosphate-buffered saline and incubated with rat anti-mouse CD34 (1:1000, eBioscience) primary antibodies overnight at 4°C. After incubation with Cy2-conjugated goat anti-rat IgG secondary antibodies and an avidin–biotin blocking step (Vector Laboratories) biotinylated rat anti-mouse F4/80 (1:300, Serotec) primary antibodies were incubated for 2 h and visualized using Cy3-conjugated Streptavidin (1:100, Biozol). The distribution of voltage-gated ion channels and the integrity of the nodes of Ranvier were determined as described previously (Kohl *et al*., 2010).

Analyses of muscle innervation in cross-sections and whole mount preparations of flexor digitorum brevis muscles were performed according to previously published protocols (Groh *et al*., 2010).

Light and fluorescence microscopic images were acquired using an Axiophot 2 microscope (Zeiss) with an attached CCD camera (Visitron Systems) or a confocal microscope (DM RE-7 SDK, Leica).

Morphometric analysis by electron microscopy

Femoral quadriceps nerves and lumbar ventral roots were processed for light and electron microscopy as previously described (Carenini *et al*., 2001; Groh *et al*., 2010). Mice at the ages of 6 and 12 months were transcardially perfused with 4% paraformaldehyde and 2% glutaraldehyde in 0.1 M cacodylate buffer. Dissected nerves were post-fixed in the same solution overnight at 4°C, followed by osmification, dehydration and embedding in Spurr's medium. Semi-thin (0.5 μm) cross-sections were stained with alkaline methylene blue for light microscopy and ultrathin sections (70 nm) were mounted to copper grids and counterstained with lead citrate for electron microscopy. Morphometric analysis was performed with a ProScan Slow Scan CCD (ProScan) camera mounted to a Leo 906 E electron microscope (Zeiss) and corresponding software iTEM (Soft Imaging System). Multiple image alignments were acquired and characteristic pathological alterations were quantified in relation to the total number of myelin competent axons in whole nerve cross-sections. For illustration of cell–cell interaction, grey scale electron micrographs have been additionally coloured using Adobe Photoshop (CS3 Version; Fig. 3D, Fig. 8, Supplementary Fig. 7).

Western blot analyses

Peripheral nerves were quickly dissected, snap frozen in liquid nitrogen and sonicated (Sonoplus HD60, Bandelin electronic) in 100 μl radioimmunoprecipitation assay lysis buffer (25 mM Tris–HCl pH 8, 10 mM Hepes, 150 mM NaCl, 145 mM KCl, 5 mM $MgCl_2$, 2 mM EDTA, 0.1% sodium dodecyl sulphate, 1% NP-40, 10% glycerol) per 10 mg tissue. Protein concentration was determined by Lowry assay (Sigma-Aldrich) and proteins were resolved by sodium dodecyl sulphate–polyacrylamide gel electrophoresis, transferred to nitrocellulose membranes and visualized using Ponceau S (Roth). Membranes were blocked with skimmed milk and probed with antibody solution overnight at 4°C (mouse anti-mouse myelin-associated glycoprotein, 1:1000, Chemicon; rabbit anti-mouse myelin basic protein, 1:1000, MBL; mouse anti-mouse myelin protein zero, 1:10 000; mouse anti-mouse β-III tubulin, 1:10 000, Chemicon). Incubation with horseradish peroxidase-conjugated secondary antibodies was performed for 1 h at room temperature and detection of the immune reaction was achieved by use of ECL reagent and ECL hyperfilm (GE Healthcare Bio-Sciences AB). Sequential stainings were performed after incubating the nitrocellulose membrane with stripping buffer (0.2 M glycine, 0.1% sodium dodecyl sulphate, 10 mM dithiothreitol, and 1% Tween) for 30–120 min. Complete removal of the first set of primary antibodies was controlled by staining with secondary antibodies.

Sural nerve biopsies

Archived diagnostic sural nerve biopsy specimens from three patients with Charcot–Marie–Tooth type 1X (Patients X1–3, Table 1) and from three patients with Charcot–Marie–Tooth type 1A (Patients A1–3, Table 1) were investigated. One additional patient with a clear family history and clinically unequivocal Charcot–Marie–Tooth type 1 refused genetic analysis so that a definite diagnosis (e.g. Charcot–Marie–Tooth type 1A) was not possible (Patient NP, Table 1). Samples of all patients were immersion-fixed and processed for semi-thin and ultrathin sections according to standard techniques (Schroder *et al*., 1985; Schmidt *et al*., 1996). Additionally, parts of samples from Patients X3 and NP were fresh frozen for preparation of 10 μm serial cryosections. For immunohistochemistry, cryosections

Table 1 Diagnostic biopsies: clinical and genetic data of the corresponding patients with Charcot–Marie–Tooth type 1

Patient	Charcot–Marie–Tooth type 1 affected gene mutation	Sex	Age at biopsy (years)	Age at onset (years)	Tissue preservation	Previously published	Source
X1	CMT1X Cx32 Arg22Gln	M	12	9	Glutaraldehyde	(Senderek *et al*., 1998, 1999)	A
X2	CMT1X Cx32 679insT	M	28	8	Glutaraldehyde	(Senderek *et al*., 1999)	A
X3	CMT1X Cx32 Pro172Ser	M	47	40 (slim ankles and feet since childhood)	Glutaraldehyde/ fresh frozen	–	W
A1	CMT1A PMP22 duplication	M	59	49	Glutaraldehyde	–	A
A2	CMT1A PMP22 duplication	F	54	26	Glutaraldehyde	–	A
A3	CMT1A PMP22 duplication	M	58	33	Glutaraldehyde	–	A
NP	CMT1[a]	F	54	53	Glutaraldehyde/ fresh frozen	–	W

a Clinical investigation and family history unequivocally identified the patient as suffering from Charcot–Marie–Tooth type 1. Since the patient refused genetic analysis, a detailed diagnosis (e.g. Charcot–Marie–Tooth type 1A) was not possible.
A = Institute of Neuropathology, RWTH Aachen University; CMT = Charcot–Marie–Tooth; W = Department of Neurology, University of Würzburg.

were post-fixed in ice-cold acetone for 10 min and blocked with 5% bovine serum albumin in phosphate-buffered saline, followed by antibody incubation and detection similar to mouse tissues. Primary antibodies included rabbit anti-human CSF-1 (1:300; Santa Cruz), mouse anti-human CD34 (1:500; eBioscience) and mouse anti-human CD68 (1:1000; Dako).

Statistical analysis

All quantifications and morphometric analyses were performed by investigators unaware of the genotypes of the respective mice. Data are represented as mean values plus standard deviations. Sample data of immune cell numbers and semi-quanitiative real-time polymerase chain reaction results were normally distributed and compared using the unpaired two-tailed Student's *t*-test. Statistical analyses of quantification of CSF-1 immunocytochemistry, cell–cell contacts, morphometric data, integrity of the nodes of Ranvier and muscle innervation were performed by use of the non-parametric Mann–Whitney U-test. *P*-values considered as significant were indicated by asterisks according to the following discrimination: $*P < 0.05$; $**P < 0.01$; $***P < 0.001$. Significant differences between Cx32wt and Cx32def genotype groups are indicated above the corresponding bars. Analyses of Cx32wt/Csf1op mice did not display any differences compared to Cx32wt mice in the described experiments and are not shown. In addition, heterozygous Csf1op/+ mice (Cx32wt/Csf1op/+ or Cx32def/Csf1op/+) did not show any differences to $Csf1^{+/+}$ mice (wild-type or Cx32def/Csf1wt) and are also not shown. Heterozygous female connexin32-deficient mice ($Cx32^{+/-}$) were not included in the experiments.

Results

CSF-1 is upregulated in peripheral nerves of connexin 32-deficient mice

In order to measure the relative levels of CSF-1 messenger RNA in peripheral nerves of wild-type and connexin 32-deficient mutants (Cx32def), we performed semi-quantitative real-time polymerase chain reaction for CSF-1 in sciatic nerves of the respective genotypes. In nerves from 6-month-old mutants, an elevation of CSF-1 messenger RNA expression levels by a factor of approximately six was detected (Fig. 1A and B).

Next, we investigated the cellular components of the peripheral nerves as possible sources for CSF-1 in wild-type and Cx32def mutant mice. By using radioactive *in situ* hybridization in combination with immunohistochemistry, we identified accumulations of silver grains on CD34-positive profiles, identifying endoneurial fibroblasts as source for CSF-1 messenger RNA in Cx32def mice. Fibroblasts from wild-type mice showed less frequent and less dense accumulation of silver grains (Fig. 1C, Supplementary Fig. 1A). Also, some weaker accumulations of CSF-1-related grains were identified on some F4/80-positive macrophages from mutant, but not from wild-type mice after longer exposure time (Fig. 1C, Supplementary Fig. 1B). Schwann cells, identified as S100β-positive profiles, were not associated with accumulations of CSF-1 messenger RNA (data not shown). These findings were confirmed by immunocytochemistry on teased nerve preparations using a CSF-1 directed antibody and fibroblast (CD34) or macrophage markers (F4/80; Fig. 1D and E). By quantification of CSF-1 producing cells, we found that in Cx32def mutants ~50% of endoneurial fibroblasts showed immunoreactivity against CSF-1, while only ~10% of macrophages were CSF-1-positive (Fig. 1F and G). Since the number of endoneurial fibroblasts is moderately higher than the number of macrophages in the myelin mutant mice (see below) and since both *in situ* hybridization signals and immunocytochemistry revealed stronger and more frequent labelling in fibroblasts, our quantitative study reveals that the vast majority of CSF-1 in the nerve is produced by these cells. Confirming specificity of the immunocytochemistry, CSF-1 was not detectable in fibroblasts (Fig. 1H) or any other cell types in peripheral nerves of homozygous osteopetrotic mice, which carry a spontaneous null mutation in the *Csf1* gene (Yoshida *et al*., 1990).

Low-level expression and immunoreactivity for CSF-1 in endoneurial fibroblasts from wild-type mice encouraged us to also investigate peripheral nerves of mice expressing nuclear localized

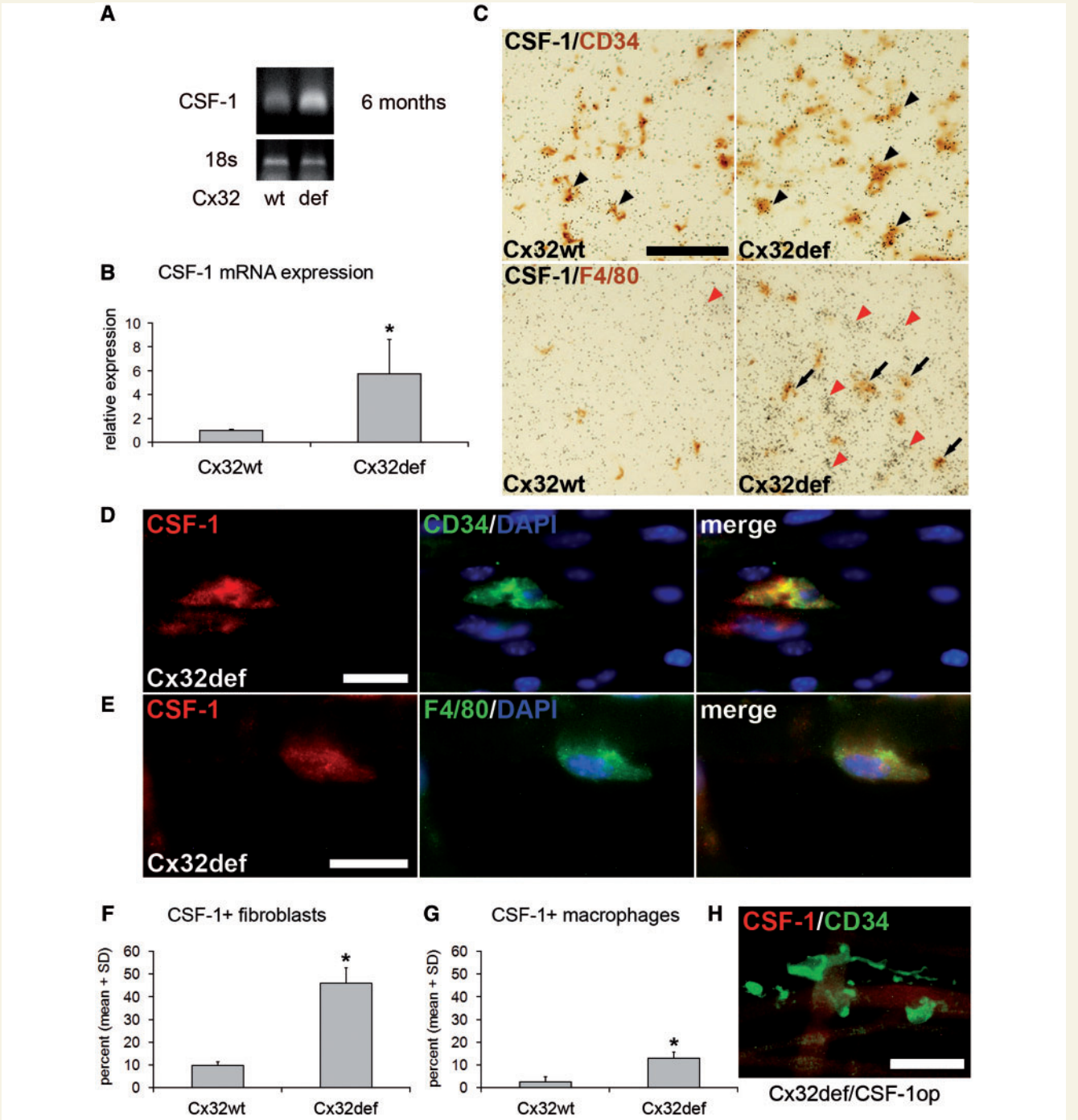

Figure 1 Increased expression of CSF-1 in peripheral nerves of Cx32def mice. (**A** and **B**) Semi-quanitiative real-time polymerase chain reaction for CSF-1 messenger RNA and 18S ribosomal RNA expression as endogenous control revealed increased CSF-1 levels in sciatic nerves from 6-month-old Cx32def mice compared with age-matched wild-type (wt) mice ($n = 4$). Student's *t*-test $^*P < 0.05$. (**C**) CSF-1 specific *in situ* hybridization in combination with immunohistochemistry against CD34 after 10 weeks (*top*) or F4/80 after 20 weeks (*bottom*) of exposure on cross-sections of femoral quadriceps nerves from 6-month-old wild-type or Cx32def mice. Arrowheads demarcate accumulations of silver grains in CD34-positive cell profiles and arrows indicate accumulations in F4/80-positive cell profiles. Note accumulation of grains on F4/80-negative 'ghost profiles', most probably representing endoneurial fibroblasts (red arrowheads) since these were the only cells showing accumulations after 10 weeks. Scale bar = 50 μm. (**D**) Double immunocytochemistry against CSF-1 (red) and CD34 (green) or (**E**) F4/80 (green) on teased nerve preparations (sciatic nerve) from 6-month-old Cx32def mice. Scale bars = 20 μm. (**F**) Quantification of CSF-1-positive (CD34-positive) fibroblasts or (**G**) CSF-1-positive (F4/80-positive) macrophages in teased nerve preparations (quadriceps nerve) from 6-month-old wild-type and Cx32def mice ($n = 3$). Note that fibroblasts are the major CSF-1-expressing cell type. Mann–Whitney U-test $^*P < 0.05$. (**H**) Double immunocytochemistry against CSF-1 (red) and CD34 (green) on teased nerve preparations (sciatic nerve) from 6-month-old Cx32def/Csf1op mice demonstrated absence of CSF-1 immunoreactivity. Scale bar = 30 μm.

β-galactosidase driven by the *Csf1* promoter (Ryan *et al*., 2001). Using X-gal histochemistry in peripheral nerves of these mutants, we again identified CD34-positive fibroblasts as sources for CSF-1, whereas Schwann cells and macrophages were not labelled (Supplementary Figs 2 and 3), corroborating our results obtained by *in situ* hybridization and immunocytochemistry by an independent method.

CSF-1 mediates increase of macrophage numbers in peripheral nerves of connexin 32-deficient mice

As reported previously, numbers of macrophages are elevated in peripheral nerves of Cx32def mice when compared with wild-type mice (Kobsar *et al*., 2003; Groh *et al*., 2010). We investigated whether this elevation is at least partially mediated by CSF-1. As a prerequisite, immunocytochemistry revealed that the cognate receptor CSF-1R (c-Fms) was expressed in peripheral nerves of Cx32wt and Cx32def nerves. The number of CSF-1R-positive cells and immunoreactivity were increased in the nerves of Cx32def mice (Fig. 2A). Double labelling confirmed that CSF-1R was exclusively expressed on endoneurial macrophages, whereas no other cell types showed CSF-1R immunoreactivity (Fig. 2B). By crossbreeding Cx32def mice with osteopetrotic mice (see above), we identified CSF-1, rather than the other known CSF-1R ligand, interleukin-34 (Wei *et al*., 2010), as the pivotal mediator of increased macrophage numbers (Fig. 2C and D), an observation comparable to our previous findings in another myelin mutant mouse, the $P0^{+/-}$ mutant (Carenini *et al*., 2001; Muller *et al*., 2007). Additionally, we observed that the attenuated increase of macrophage numbers in Cx32def nerves in the absence of CSF-1 was not a transient effect, but persisted until the age of 12 months, the latest time point investigated (Fig. 2E). Of note, both increase of F4/80-positive and myelin-phagocytosing macrophage numbers was blocked, as revealed by immunocytochemistry and electron microscopy, respectively (Fig. 2F and G). Furthermore, and comparable to previous observations in $P0^{+/-}$ mice (Carenini *et al*., 2001), the number of T-lymphocytes—typically present in mutant nerves—was significantly reduced in the absence of CSF-1 (Supplementary Fig. 4).

CSF-1-producing fibroblasts form cell–cell contacts with macrophages

After having identified endoneurial fibroblasts as a cellular source of CSF-1 that mediates increase of macrophage numbers in the mutants, we investigated the spatial interrelationships between endoneurial fibroblasts and macrophages in wild-type and mutant mice. By double immunofluorescence, F4/80-positive macrophages and CD34-positive fibroblasts could often be found in close contact with each other (Fig. 3A). Furthermore, quantification of double immunofluorescence revealed that ~60% of F4/80-positive macrophages directly contacted CD34-positive fibroblasts in wild-type and Cx32def mice (Fig. 3B). Of note, the absolute numbers of both fibroblasts (Fig. 3C) and macrophages (see above) were elevated in the Cx32def mutants. Interestingly, however, in Cx32def/Csf1op mutants, macrophage (see above), but not fibroblast (which do not express CSF-1R, see above) numbers, are decreased in the absence of CSF-1 (Fig. 3C). As a likely consequence, significantly more macrophages (~80%) were found in direct contact with fibroblasts compared to wild-type or Cx32def nerves (Fig. 3B). In order to further investigate the intimate contact between fibroblasts and macrophages we performed electron microscopy of ultrathin serial sections. 'Foamy' macrophages containing myelin debris or lipid vacuoles were often found in proximity to thinly myelinated or demyelinated axons and were frequently in direct cell–cell contact with fibroblasts identified by long basal lamina-free endoneurial processes and staggered rough endoplasmic reticulum (Fig. 3D–F). Serial sections through such a cellular assembly demonstrated that contacts between macrophages and fibroblasts are not restricted to small proportions of the cells, but extend over large aspects of the cell surface (Fig. 3D1–4).

CSF-1 deficiency leads to a substantial and persistent amelioration of the demyelinating and axonopathic phenotype in connexin 32-deficient mice

We have previously shown that in another model for Charcot–Marie–Tooth type 1 disorders, $P0^{+/-}$ mice, lack of CSF-1 leads not only to blocked increase of macrophage numbers, but also to strongly reduced myelin degeneration (Carenini *et al*., 2001). Here, we demonstrate a similar alleviation of demyelinating phenotype in another model, Cx32def mice. As another novel finding, we show that the rescue effect of CSF-1 deficiency is highly persistent: not only peripheral nerves from 6-, but also from 12-month-old Cx32def mice lacking CSF-1 showed substantially reduced pathological alterations with minimal tendency of further demyelination. This profound rescue effect was detected by light microscopy and electron microscopic quantification of lumbar ventral roots (Fig. 4A, Supplementary Fig. 5) and femoral quadriceps nerves (Figs 4B and 5A–D). Furthermore, immunoblot analyses for myelin protein levels in sciatic nerve lysates were in line with a substantial preservation of myelin in the absence of CSF-1 (Fig. 4C). Thus, lack of CSF-1 strongly and persistently improves myelin maintenance. In addition to improved myelin integrity, formation of axonopathic alterations characteristic of Cx32def mice, namely periaxonal vacuoles and regeneration clusters, was persistently reduced in the absence of CSF-1 (Fig. 5E–H).

We additionally focused our attention on two functionally important compartments: the nodal regions and the neuromuscular junction.

As revealed by immunocytochemistry on single fibre preparations, Cx32def mice showed normal nodal and paranodal compartments, as reflected by the distribution of voltage-gated $Na+$ channels (Nav1.6) and Caspr-immunoreactivity, respectively (Fig. 6A). By contrast, the juxtaparanodal compartment constantly showed abnormal 'patchy' domains of voltage-gated K^+ channel

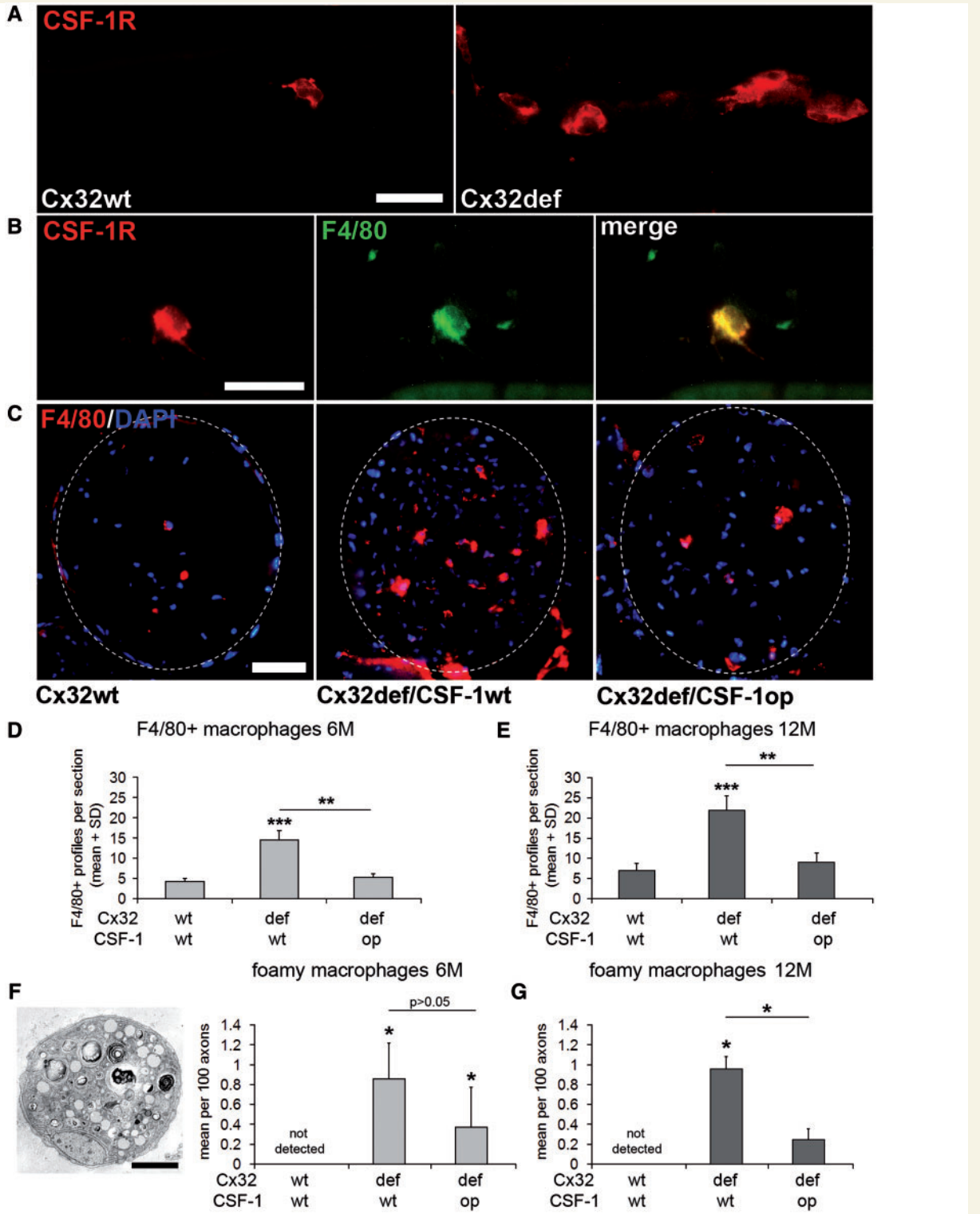

Figure 2 CSF-1 mediates increase of macrophage numbers in peripheral nerves of Cx32def mice. (**A**) Immunocytochemistry against CSF-1R (c-Fms; red) on teased nerve preparations (sciatic nerve) from 6-month-old wild-type and Cx32def mice. Scale bar = 30 μm. (**B**) Double immunocytochemistry against CSF-1R (red) and F4/80 (green) on teased nerve preparations (sciatic nerve) from 6-month-old Cx32def mice. All CSF-1R-positive cell profiles were F4/80-positive macrophages. Scale bar = 30 μm. (**C**) Immunohistochemistry against F4/80-positive macrophages in cross-sections of femoral quadriceps nerves from 6-month-old wild-type, Cx32def/Csf1wt and Cx32def/Csf1op mice. Broken lines demarcate the boundaries of quadriceps nerves. Scale bar = 50 μm. (**D**) Quantification of F4/80-positive macrophages in 6-month-old (n = 4–5) and (**E**) 12-month-old (n = 3–4) Cx32/Csf1 mutants revealed attenuated elevation of macrophage numbers in Cx32def/Csf1op compared with Cx32def/Csf1wt quadriceps nerves. Student's t-test $^{**}P < 0.01$; $^{***}P < 0.001$. (**F**) Electron microscopy and quantification of foamy macrophages in quadriceps nerves from 6-month-old (n = 4) and (**G**) quantification of foamy macrophages in quadriceps nerves from 12-month-old (n = 3–4) Cx32/Csf1 mutants. Scale bar = 2 μm. Mann–Whitney U-test $^{*}P < 0.05$.

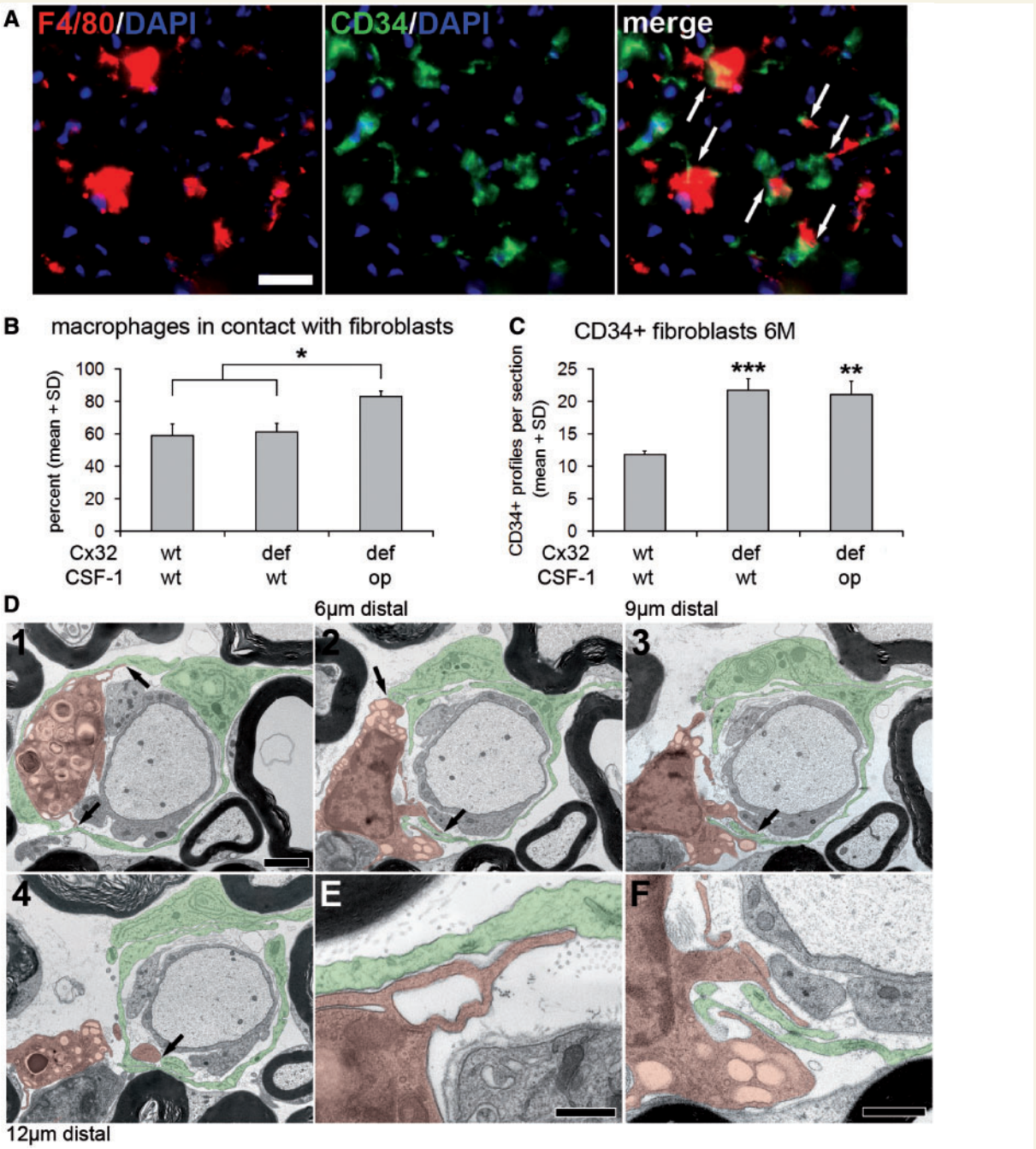

Figure 3 Endoneurial fibroblasts form direct cell–cell contacts with macrophages. (**A**) Double immunohistochemistry against F4/80 (red) and CD34 (green) on cross-sections of quadriceps nerves from 6-month-old Cx32def/Csf1wt mice. Arrows indicate cell–cell contacts between macrophages and fibroblasts. Scale bar = 20 µm. (**B**) Quantification of F4/80-positive macrophages in contact with CD34-positive fibroblasts in quadriceps nerves of 6-month-old wild-type, Cx32def/Csf1wt and Cx32def/Csf1op mice ($n = 4$). Percentages of macrophages in contact with fibroblasts were similar in wild-type and Cx32def/Csf1wt nerves, but significantly increased in Cx32def/Csf1op nerves. Mann–Whitney U-test, $*P < 0.05$. (**C**) Quantification of CD34-positive endoneurial fibroblasts revealed a significant increase in numbers in both Cx32def/Csf1wt and Cx32def/Csf1op mice compared with wild-type mice ($n = 4$). Student's *t*-test, $**P < 0.01$; $***P < 0.001$. (**D1–4**) Electron micrographs of ultrathin serial sections (70 nm thick; over 12 µm) of lumbar ventral roots from a 6-month-old Cx32def/Csf1wt mouse. A 'foamy' macrophage (orange) containing myelin debris was found in close proximity to a demyelinated axon and in direct cell-cell contact (arrows) with fibroblast processes (green) at several sites. Scale bar = 2 µm. (**E** and **F**) Higher magnification of the macrophage-fibroblast contact sites as shown in **D1** and **D2**. Note the membrane-to-membrane association of macrophage and fibroblast processes. Scale bars = 0.5 µm in **E**; 1 µm in **F**.

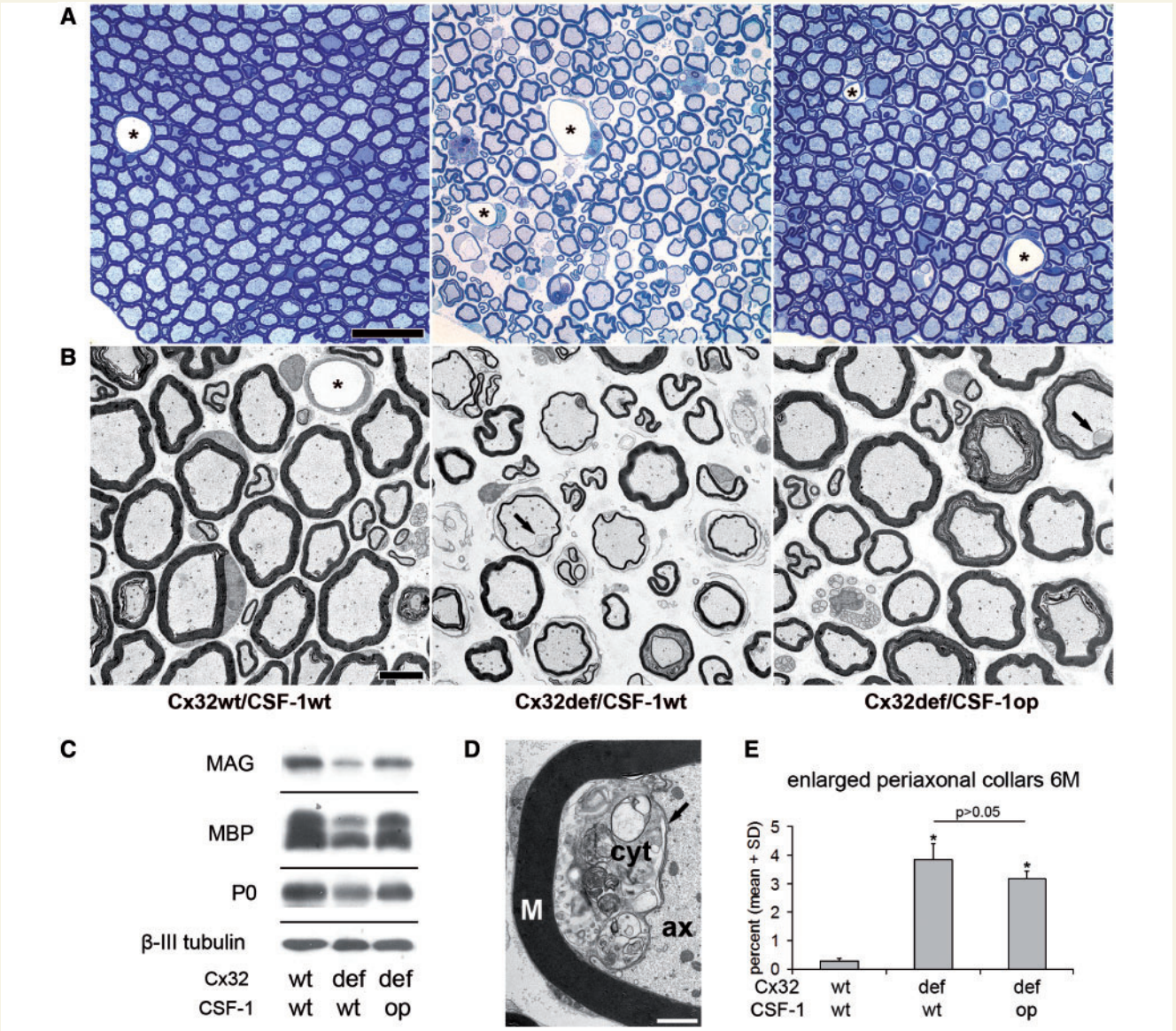

Figure 4 CSF-1 deficiency leads to a substantial amelioration of neuropathy in peripheral nerves of Cx32def mice. (**A**) Light microscopy of representative semithin sections of lumbar ventral roots and (**B**) electron microscopy of representative ultrathin sections of femoral quadriceps nerves from 12-month-old wild-type, Cx32def/Csf1wt and Cx32def/Csf1op mice. Note prominent pathological alterations in Cx32def/Csf1wt mice, such as abnormally myelinated (thinly myelinated and demyelinated) axons, onion bulbs, periaxonal vacuoles and regeneration clusters. Such features were rarely seen in Cx32def/Csf1op mice and most of the myelinated profiles appeared nearly normal. Enlarged periaxonal collars (arrows) were amply present in both genotypes. Asterisks demarcate blood vessels. Scale bars = 20 μm in **A**; 5 μm in **B**. (**C**) Western blot analysis for the myelin proteins myelin-associated glycoprotein (MAG), myelin basic protein (MBP) and myelin protein zero (MPZ;P0) (and β-III tubulin as loading control) in sciatic nerve lysates from 12-month-old wild-type, Cx32def/Csf1wt and Cx32def/Csf1op mice. All analysed myelin proteins showed strongly reduced levels in sciatic nerves from Cx32def/Csf1wt mice compared with wild-type nerves, but only mildly reduced levels in nerves from Cx32def/Csf1op mice. (**D**) Electron microscopy of an enlarged periaxonal collar. The Schwann cell collar (arrow) filled with cytoplasm (cyt) containing vesicular inclusions protrudes into the axonal space (ax). M = myelin; scale bar = 1 μm. (**E**) Morphometric quantification of enlarged periaxonal collars in femoral quadriceps nerves from 6-month-old wild-type, Cx32def/Csf1wt and Cx32def/Csf1op mice ($n = 4$) failed to demonstrate a dependency of this mutation-specific hallmark from CSF-1 expression. Mann–Whitney U-test. $P > 0.05$.

(Kv1.2) immunoreactivity (Fig. 6A). The formation of these abnormal domains was reduced in the absence of CSF-1 (Fig. 6B), reflecting an ameliorated phenotype at the juxtaparanodal level.

We also investigated flexor digitorum brevis muscles with regard of the preservation of neuromuscular junctions. Denervation of neuromuscular junctions in Cx32def mice was identified in whole mount preparations and cross-sections of muscles (Fig. 6C).

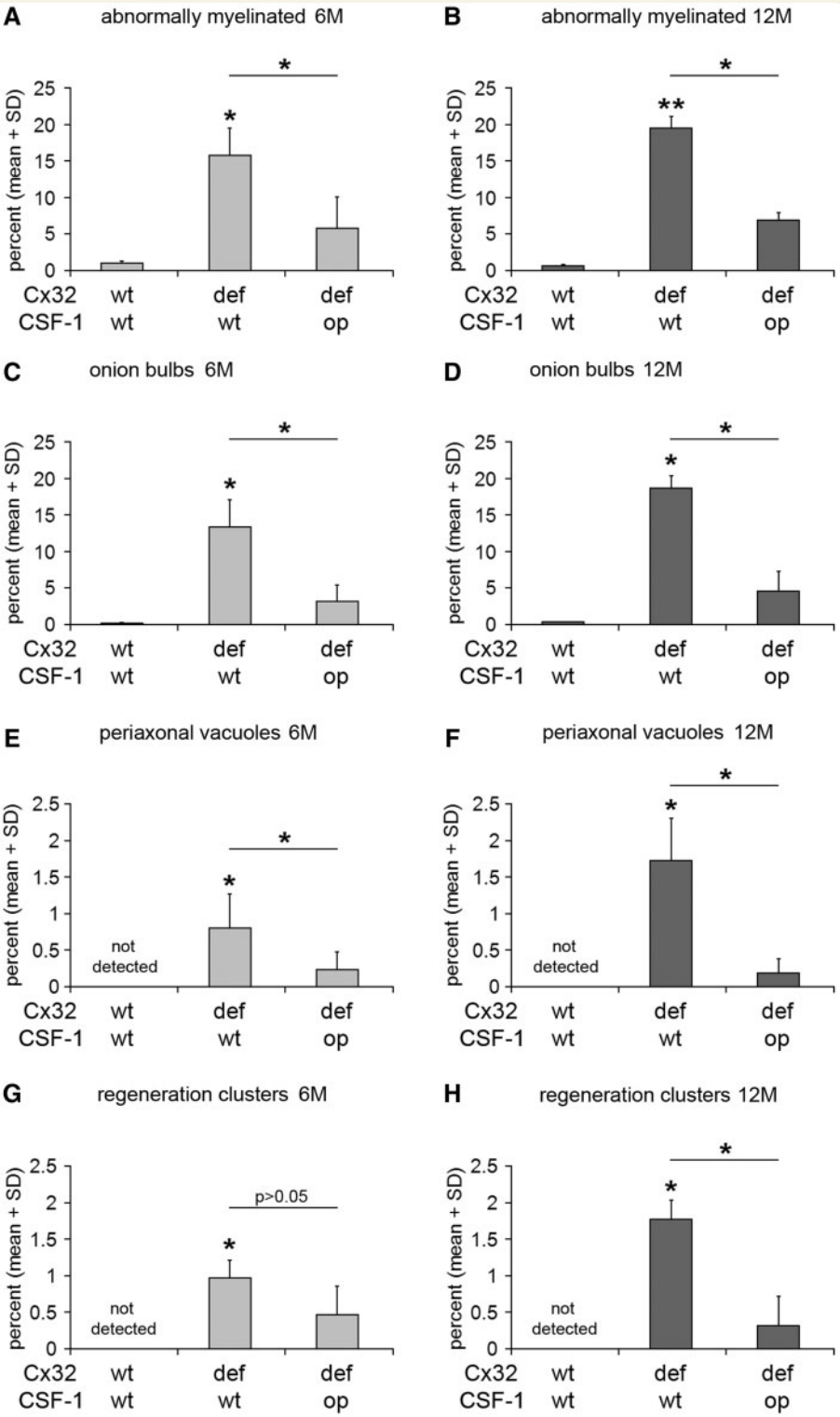

Figure 5 CSF-1 deficiency leads to persistent amelioration of the demyelinating and axonopathic phenotype in peripheral nerves of Cx32def mice. (**A**, **C**, **E** and **G**) Morphometric quantification of abnormally myelinated (thinly myelinated and demyelinated) axons, onion bulb profiles, periaxonal vacuoles and regeneration clusters by electron microscopy of femoral quadriceps nerves from 6-month-old (6M) ($n = 4–5$) and (**B**, **D**, **F** and **H**) 12-month-old (12M) ($n = 3–4$) wild-type, Cx32def/Csf1wt and Cx32def/Csf1op mice. Formation of alterations in myelin integrity (abnormally myelinated axons and onion bulbs) in Cx32def mice was significantly ameliorated in the absence of CSF-1 at 6 and 12 months of age. Formation of axonopathic alterations in Cx32def mice in form of periaxonal vacuoles was significantly ameliorated in the absence of CSF-1 at 6 and 12 months of age, while attenuation in the formation of regeneration clusters (axonal sprouting after damage) reached significance only at 12 months of age. Mann–Whitney U-test, $*P < 0.05$; $**P < 0.01$. Note that Cx32def/Csf1op mice show no or only minimal increase in the formation of neuropathic alterations between 6 and 12 months of age.

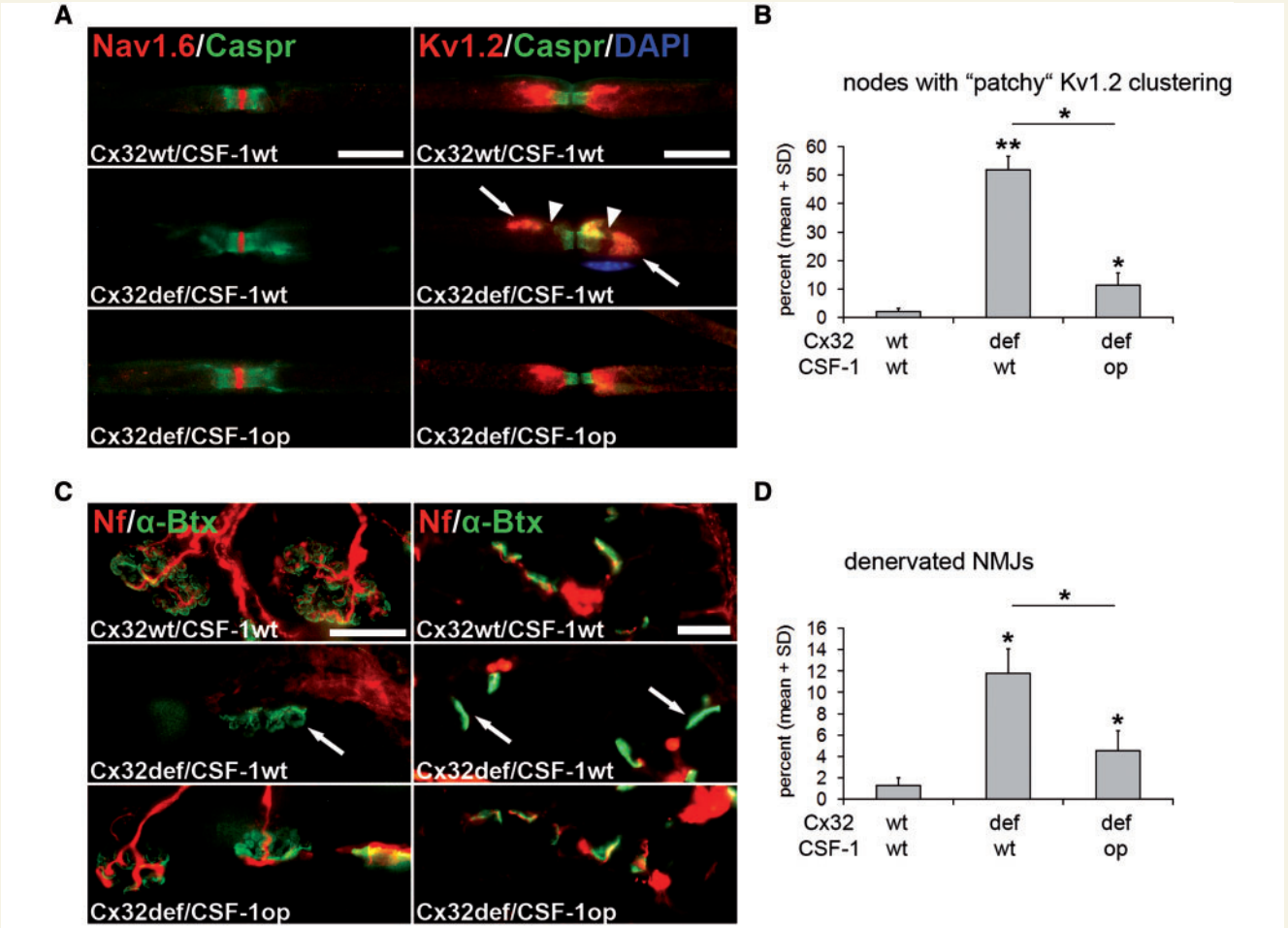

Figure 6 CSF-1 deficiency leads to reduced formation of maldistributed juxtaparanodal ion channels and reduced denervation of neuromuscular junctions in Cx32def mice. (**A**) Double immunocytochemistry against voltage-gated Na^+ channels (Nav1.6; red) or voltage-gated K^+ channels (Kv1.2; red) in combination with Contactin-associated protein (Caspr; green) on teased fibre preparations of quadriceps nerves from 6-month-old wild-type, Cx32def/Csf1wt and Cx32def/Csf1op mice. Nodal (Nav1.6) and paranodal (Caspr) domains appeared normally organized in mice of all genotypes, while juxtaparanodal K^+ channels frequently presented with 'patchy' maldistribution in nerves from Cx32def/Csf1wt mice (arrows). This abnormal distribution of K^+ channels causes 'gaps' in the immunopositive aspects (arrowheads) and is substantially reduced in the absence of CSF-1. Note the nucleus of an unidentified cell (a putative macrophage) in proximity to the abnormal juxtaparanodal domain. Scale bars = 20 μm. (**B**) Quantification of nodes of Ranvier with 'patchy' K^+ channel distribution in quadriceps nerves from 6-month-old wild-type, Cx32def/Csf1wt and Cx32def/Csf1op mice (n = 3–5) revealed reduced formation of 'patchy' clustering in Cx32def mice in the absence of CSF-1. Mann–Whitney U-test $*P < 0.05$; $**P < 0.01$. (**C**) Visualization of neurofilament-positive (red) presynaptic axon terminals and α-bungarotoxin-positive (green) postsynaptic terminals in whole mount preparations (*left*) or cross-sections (*right*) of flexor digitorum brevis muscles from 12-month-old wild-type, Cx32def/Csf1wt and Cx32def/Csf1op mice. Arrows demarcate neurofilament-negative, denervated (or partially denervated) postsynapses. Scale bars = 30 μm. (**D**) Quantification of denervated neuromuscular junctions (NMJs) in cross-sections of flexor digitorum brevis muscles from 12-month-old wild-type, Cx32def/Csf1wt and Cx32def/Csf1op mice (n = 3–4) revealed reduced denervation in Cx32def mice in the absence of CSF-1. Mann–Whitney U-test, $*P < 0.05$.

We found ~12% of α-bungarotoxin-positive postsynaptic terminals lacking neurofilament-positive presynaptic profiles in cross-sections of 12-month-old Cx32def mice, reflecting a typical dying-back neuropathy and corroborating previous results (Groh *et al*., 2010). However, in the absence of CSF-1, only 4% of α-bungarotoxin-positive postsynaptic terminals were devoid of presynaptic terminals in Cx32def mice, thus resembling neuromuscular junctions of wild-type mice (Fig. 6D).

We also intended to investigate the functional consequences of preserved axon and neuromuscular integrity in Cx32def/Csf1wt versus Cx32def/Csf1op mutants as in related studies (Groh *et al*., 2010). However, due to the substantially smaller size and generally less vital appearance of the Csf1op mutants (Yoshida *et al*., 1990; Ryan *et al*., 2001), both electrophysiological recordings and the determination of muscle strength failed to deliver reliable results.

CSF-1 is expressed by macrophage-contacting endoneurial fibroblasts in peripheral myelin protein 22-overexpressing mutants

Since CSF-1 plays a pivotal role in the activation of pathogenic macrophages in models for Charcot–Marie–Tooth types 1X (this study) and 1B (Carenini *et al*., 2001), we also investigated the cellular expression of the cytokine in PMP22-overexpressing mutants (strain C61), a model for the most common form of inherited neuropathies, Charcot–Marie–Tooth type 1A (Huxley *et al*., 1998). As shown in Supplementary Fig. 6, there was a strong elevation in the number of both F4/80-positive macrophages (Supplementary Fig. 6A) and CD34-positive endoneurial fibroblasts (Supplementary Fig. 6B) in quadriceps nerves of PMP22-overexpressing mice. Moreover, ~60% of the F4/80-positive macrophages made close contact with CD34-positive fibroblasts (Supplementary Fig. 6C). Double immunocytochemistry revealed that similar to Cx32def mice, CSF-1 in the nerves of PMP22tg mice was mostly expressed by CD34-positive fibroblasts (Supplementary Fig. 6D). These observations strongly suggest that fibroblast-borne expression of CSF-1 is a widespread phenomenon in mouse models for Charcot–Marie–Tooth type 1.

Endoneurial fibroblasts in human sural nerve biopsies from patients with Charcot–Marie–Tooth type 1X and type 1A express CSF-1 and contact macrophages

After having shown that CSF-1 mediates demyelination in at least two Charcot–Marie–Tooth type 1 models and appears to be uniformly expressed by macrophage-contacting endoneurial fibroblasts, we investigated CSF-1 expression in sural nerve biopsies from patients with Charcot–Marie–Tooth type 1X and patients with type 1A. Indeed, in the only cryopreserved biopsy available from a patient with Charcot–Marie–Tooth type 1X (Table 1, Patient X3) immunohistological investigations on consecutive cryosections revealed cell–cell contacts between CD34-positive endoneurial fibroblasts and CD68-positive macrophages (Fig. 7A). Furthermore, double immunohistochemistry against CD34 or CD68 and CSF-1 revealed that predominantly endoneurial fibroblasts, rather than macrophages, expressed CSF-1 (Fig. 7B and C). Interestingly, ~55% of CD68-positive macrophages contacted CSF-1-positive cells (predominantly endoneurial fibroblasts), which is comparable to our findings in mice (see above). Electron microscopy on a glutaraldehyde-fixed portion of the biopsy from the same patient revealed abundant cell–cell contacts between morphologically identified fibroblasts and macrophages and, occasionally, myelin-laden macrophages in close contact with demyelinated axons (data not shown), reminiscent of observations in our Charcot–Marie–Tooth type 1 mutants and some other biopsies (Crawford and Griffin, 1991; Carvalho *et al*., 2005). We then extended our studies on two other patients with Charcot–Marie–Tooth type 1X (Patients X1 and 2), the biopsies of which were glutaraldehyde-fixed. On electron micrographs of these patients, contacts between morphologically identified fibroblasts and macrophages were found repeatedly (Fig. 8A and Supplementary Fig. 7A). We found that 20–30% of the macrophages were in contact with endoneurial fibroblasts, which is lower than the values obtained by immunohistochemical methods (see above). This is most likely due to the fact that during our electron microscopic evaluation, we excluded cell profiles that could not be unequivocally identified as macrophages or fibroblasts. Macrophages were identified by their finger-like/microvillar processes and/or the phagocytosed material as well as prominent lysosomes and phagolysosomes. Endoneurial fibroblasts were defined as cells devoid of basal lamina, microvillar processes and phagocytosed material showing extended processes and in many cases a prominent rough endoplasmic reticulum (Ohara *et al*., 1986; Grehl and Schroder, 1991).

As a final step, we investigated the source of CSF-1 in cryopreserved biopsies from a patient with clinically identified Charcot–Marie–Tooth type 1 disease, most likely not suffering from type 1X (Patient NP; Table 1). Again, CSF-1 was predominantly fibroblast-derived and the endoneurial fibroblasts were often contacting macrophages (not shown). The glutaraldehyde-fixed biopsy of a patient with genetically identified Charcot–Marie–Tooth type 1A (Patient A1) revealed frequent contacts between macrophages and endoneurial fibroblasts (Fig. 8B and Supplementary Fig. 7B). Interestingly, in this patient, morphologically identified macrophages were often integrated into onion bulbs, which is in line with observations by Stoll *et al*. (1998) showing individual cell profiles of MHC class II immunoreactivity integrated in onion bulb formations.

Discussion

Robust rescue of peripheral nerve pathology by CSF-1 inactivation

In the present study, we show a robust and persistent rescue of demyelination, axonopathic changes and presynaptic axon loss in an animal model for Charcot–Marie–Tooth type 1X by inactivating the expression of CSF-1, a cytokine involved in the differentiation and activation of various tissue macrophages, Kupffer cells, microglial cells and osteoclasts (Raivich *et al*., 1999; Kalla *et al*., 2001; Chitu and Stanley, 2006). This rescue is not due to a general absence or damage of tissue macrophages in the peripheral nerves of osteopetrotic mice, but is likely due to impaired activation and development of pathogenetic features of resident macrophages in the absence of CSF-1 (Carenini *et al*., 2001; Muller *et al*., 2007; Kondo *et al*., 2011). A similarly profound rescue of neuropathy has been demonstrated in another model for Charcot–Marie–Tooth disease, i.e. in mice heterozygously deficient in the myelin protein P0, resembling some forms of Charcot–Marie–Tooth type 1B (Carenini *et al*., 2001; Muller *et al*., 2007). Interestingly, neural preservation has also been seen in a model for Charcot–Marie–Tooth type 1A, i.e. in transgenic mice overexpressing PMP22 (strain C61), when crossbred to osteopetrotic

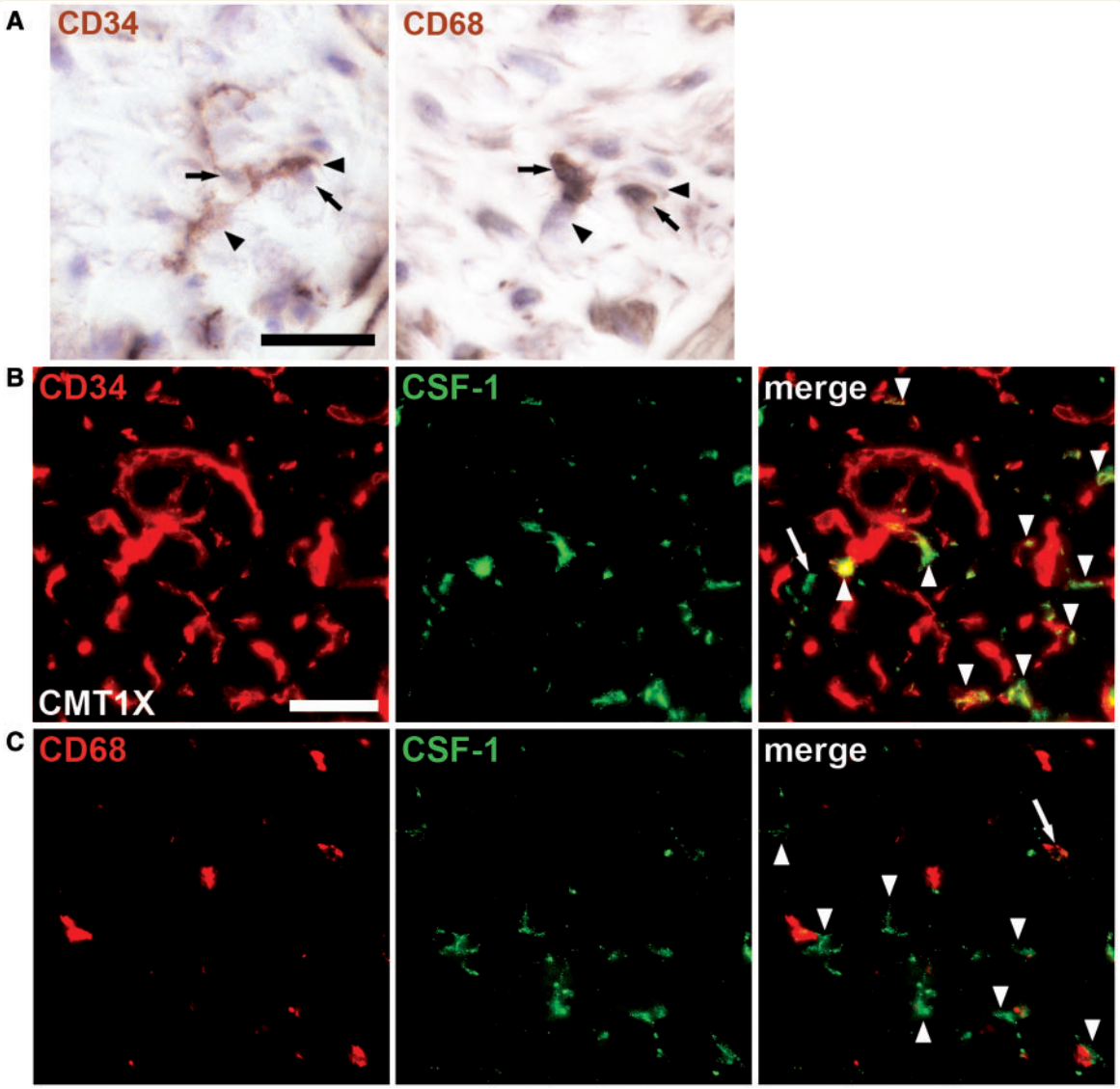

Figure 7 CSF-1-producing fibroblasts are in close contact with macrophages in peripheral nerves of human patients with Charcot–Marie–Tooth type 1. (**A**) Immunohistochemistry against CD34-positive endoneurial fibroblasts (*left*; arrowheads) and CD68-positive macrophages (*right*; arrows) in adjacent serial sections of a frozen sural nerve biopsy from a 47-year-old patient with Charcot–Marie–Tooth type 1X (Table 1, Patient X3) counterstained with haematoxylin. Fibroblasts were in close contact with cells that were identified as macrophages in the adjacent section and vice versa. Scale bar = 20 μm. (**B**) Double immunohistochemistry against CD34 (red) and CSF-1 (green) on sections of the same biopsy as shown in **A**. The majority of CSF-1-positive profiles were CD34-positive fibroblasts (arrowheads) while only few profiles, putative macrophages, did not colocalize with CD34 (arrow). Scale bar = 30 μm. (**C**) Double immunohistochemistry against CD68 (red) and CSF-1 (green) confirmed that only few macrophages were CSF-1-positive (arrow) while the majority of CSF-1-positive profiles, putative fibroblasts (arrowheads), were not CD68-positive but located in close proximity to macrophages.

mutants (Groh *et al*., in preparation). These combined observations suggest that CSF-1 serves as a common, pathologically relevant cytokine in inherited demyelination. Furthermore, the present study substantially extends the published observations made in the P0 mutants. For instance, we could demonstrate that the rescue effect is robust and persistent, lasting for at least 12 months, the latest time point investigated. Third, we show here not only myelin-related rescue, but most importantly, a robust structural, molecular and functional axonal preservation by quantification of axonopathic alterations, ion channel distribution and muscle innervation. Since axonopathic changes including muscle denervation are most relevant for the clinical outcome in patients (Berciano *et al*., 2000; Gallardo *et al*., 2006; Scherer and Wrabetz, 2008; Nave, 2010), inactivation of CSF-1 or its receptor signalling might be highly promising goals for treatment strategies in possibly several forms of Charcot–Marie–Tooth disease. Interestingly, an orally applicable and CSF-1R specific tyrosine kinase inhibitor has recently been shown to suppress development and progression of different inflammatory disease models (Ohno *et al*., 2006, 2008; Uemura *et al*., 2008).

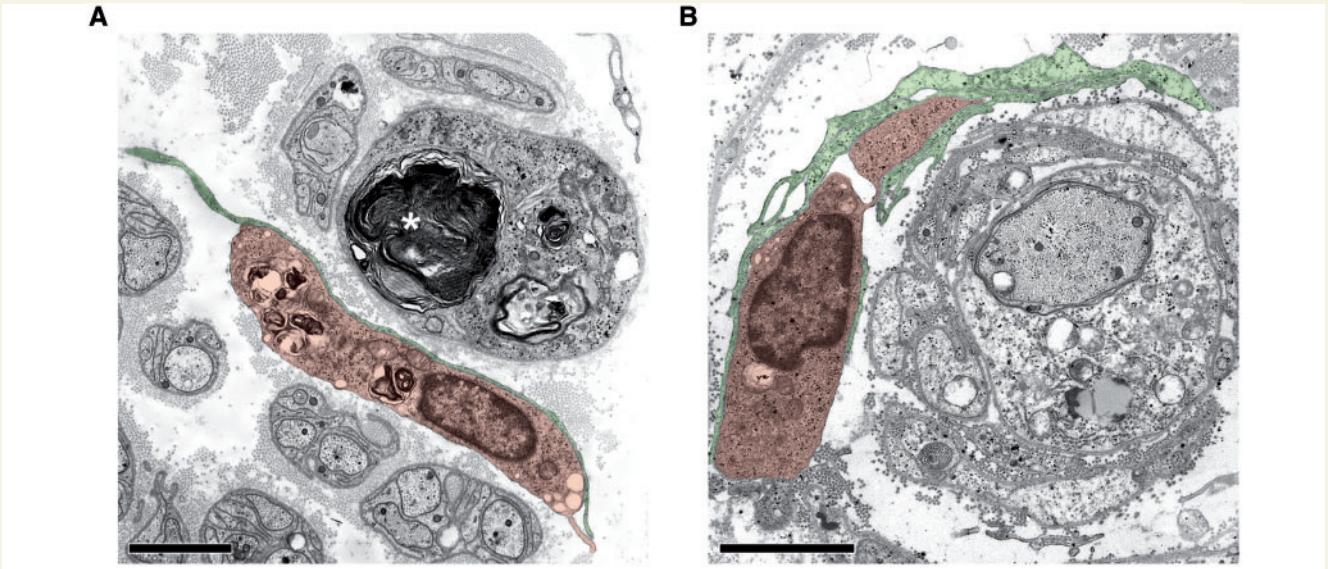

Figure 8 Endoneurial fibroblasts form direct cell–cell contacts with macrophages in human patients with Charcot–Marie–Tooth type 1. (**A**) Electron microscopy of a direct cell–cell contact between a fibroblast process (green) and a macrophage containing myelin debris (orange) in a sural nerve biopsy from a patient with Charcot–Marie–Tooth type 1X (Patient X2, Table 1). Note myelin debris in an endoneurial tube devoid of an axon (asterisk). Scale bar = 1.5 μm. (**B**) Electron microscopy of direct cell–cell contacts between fibroblast processes (green) and a macrophage (orange) in proximity to a demyelinated axon in a sural nerve biopsy from a patient with Charcot–Marie–Tooth type 1A (Patient A1, Table 1). Note that the associated macrophage-fibroblast unit is surrounding the demyelinated axon and Schwann cells profiles reminiscent of onion bulbs. Scale bar = 1.5 μm.

Of note, inactivation of CSF-1 and thus of macrophage-like cells appears not to be always beneficial; in twitcher mice characterized by impaired activity of the lysosomal enzyme galactocerebrosidase and representing globoid cell leukodystrophy, absence of CSF-1 attenuated macrophage-dependent removal of myelin debris. This has detrimental consequences for regenerative activities in the CNS of the mutants due to the blockade of migrating oligodendrocyte precursor cells by myelin (Kondo *et al*., 2011). This and our present observations exemplify that neuroinflammation can be beneficial in some diseases (see also Kerschensteiner *et al*., 1999; Hohlfeld *et al*., 2000; Linker *et al*., 2010), but detrimental in others (Ip *et al*., 2006*a*, *b*; Martini *et al*., 2008).

Fibroblasts as mediators of nerve pathology by CSF-1 expression

Apart from the robust rescue effect in inherited demyelination, our study reveals for the first time endoneurial fibroblasts as major source for CSF-1 and, thus, identifies them as important cellular contributors to an incurable nerve disorder. Three independent approaches comprising *in situ* hybridization, immunocytochemistry and X-gal-reactivity driven by the CSF-1 promoter unequivocally attributed the majority of CSF-1 expression to these cells. This defines the endoneurial fibroblast as a pathogenetically highly relevant cell in comparison to its so far established and less significant role as major provider of endoneurial collagen (Peters *et al*., 1991). Of note, the origin of endoneurial fibroblasts may not be uniform, since one group suggests their embryonic origin from neural crest (Joseph *et al*., 2004), whereas our transplantation experiments performed in adult mice revealed an origin from bone marrow (Mäurer *et al*., 2003), suggesting their relationship to blood-borne fibrocytes (Abe *et al*., 2001; Herzog and Bucala, 2010). A further feature supporting a bone marrow origin is the expression of the haematopoietic stem cell marker CD34. Another fibroblast-like cell expressing this marker is the 'kranocyte' capping the neuromuscular junction (Court *et al*., 2008). However, neither the origin of these cells nor their possible contribution to neuropathic changes has been investigated. A remarkable feature of the CD34-positive endoneurial fibroblast is their close membrane-to-membrane association with macrophages. Of note, in Cx32, PMP22 (this study) and in P0 mutants (unpublished observations) ~60% of all endoneurial macrophages are in direct contact with endoneurial fibroblasts. A similar association can be recognized on electron micrographs of peripheral nerves of rabbits under injury conditions (Thomas, 1964, 1966) and a detailed description of cell–cell contacts between the two cell types has been described for Wallerian degeneration in the mouse (Ohara *et al*., 1986). In case of inherited neuropathies and possibly other pathological conditions, the endoneurial fibroblasts can deliver CSF-1 directly to the macrophages which then attack the mutant myelin. In this context, it is striking that for the first time, fibroblast-macrophage contacts have been detected by us in biopsies of patients with Charcot–Marie–Tooth type 1A and type 1X, suggesting a similar role of this so far poorly recognized cell–cell contact in humans. With regard to this newly detected, although frequent cell-to-cell

association, it is of particular interest that in addition to two secreted isoforms, CSF-1 can be expressed as biologically active cell surface glycoprotein that mediates distinct macrophage-related functions in the organism (Dai *et al.*, 2004; Chitu and Stanley, 2006). It is therefore plausible to assume that the direct cell–cell contact between both cell partners is a prerequisite for the effective and constant activation of CSF-1R expressing macrophages by fibroblast-membrane-bound CSF-1 in the chronically diseased nerve.

The tight cell–cell association between CSF-1 'donors' and 'recipients' is well established in the bone system; the osteoblast, a specialized fibroblast-like cell, is in tight contact with the bone-related macrophage-like cell partner, the osteoclast. This association is necessary for osteoclastic bone resorption via CSF-1 produced by the osteoblast (Teitelbaum, 2000), as reflected by the osteopetrotic phenotype of spontaneous CSF-1-null mutants (Yoshida *et al.*, 1990). Another important regulatory mechanism for osteoclastogenesis is mediated by the receptor activator of nuclear factor-κB (RANK) and its ligand RANK-L. Interestingly, these interacting partners are also found in the peripheral nerve, with, in analogy to the bone, RANK-L expressed by fibroblasts and RANK by macrophages (Zieger, Groh and Martini, unpublished results). In case these molecules also contribute to detrimental macrophage function in the diseased peripheral nerve, the use of the natural RANK-L competitor osteoprotegerin or RANK-L-specific antibodies might be an option for Charcot–Marie–Tooth treatment as has been proposed for treating osteoporosis (Trouvin and Goeb, 2010).

Low-grade inflammation in demyelinating peripheral nerves is mediated by CCL2 and CSF-1

Our group has identified low-grade inflammatory reactions in peripheral nerves as important disease mediator and modifier in models for inherited demyelination (Ip *et al.*, 2006*b*; Martini *et al.*, 2008). According to our studies in three distinct models, the initial changes recorded in the mutant Schwann cell include the activation of the MEK/ERK-pathway resulting in the expression of CCL2 (MCP-1), a chemokine involved in macrophage attraction and function (Fischer *et al.*, 2008*a*, *b*; Martini *et al.*, 2008; Groh *et al.*, 2010; Kohl *et al.*, 2010). In these models, reduction of levels of CCL2 by 50% result in a similar amelioration of disease as CSF-1-deficiency, reflecting the involvement of at least two components of the innate immune system in inherited demyelination: one derived from the diseased Schwann cell (CCL2), the other from the endoneurial fibroblast (CSF-1). In line with this model is the independence of MEK-ERK signalling and CCL2 expression from CSF-1 expression: peripheral nerves from Cx32def/Csf1op mice still showed increased phosphorylation of ERK and increased CCL2 immunoreactivity in Schwann cells (Groh and Martini, unpublished results). Whereas it is not difficult to imagine that the diseased Schwann cell itself is the source of the pathogenic mediator (CCL2), elevation of a fibroblast-borne cytokine (CSF-1) in a primarily Schwann cell-related disorder appears more challenging to explain. One possibility to 'activate' endoneurial fibroblasts could occur via Schwann cell-derived CCL2. However, we have presently no evidence in favour of the expression of the cognate CCL2 receptor (CCR2) on endoneurial fibroblasts (Groh and Martini, unpublished results). We, therefore, favour the hypothesis that macrophages activated by Schwann cell-borne CCL2 communicate to the closely attached endoneurial fibroblasts, which then 'signal back' to the macrophage by CSF-1 expression. This model is complicated by the fact that complete CCL2 inactivation results in an aggravated phenotype, which is likely mediated by a robust upregulation of CSF-1 (Fischer *et al.*, 2008*a*, *b*; Groh *et al.*, 2010; Kohl *et al.*, 2010). Recent observations could again identify the endoneurial fibroblasts as source for CSF-1 under these conditions (Groh and Martini, unpublished observation). It is, therefore, plausible to assume that CCL2 serves as a Schwann cell-derived, disease modulator which either when elevated or completely inactivated leads to detrimental upregulation of fibroblast-borne CSF-1.

Conclusions

In the present study, we identified fibroblast-borne CSF-1 upregulation as an important disease mediator in a model for a non-curable inherited peripheral neuropathy. Since this mechanism is not confined to the Charcot–Marie–Tooth type 1X model, but is also realized in at least two other models ($P0^{+/-}$, Carenini *et al.*, 2001; PMP22tg, this study), fibroblast-borne CSF-1 is a common and widespread promoter of pathogenesis in inherited demyelination of distinct genetic origin. Based on our present observations in human biopsies that at least in Charcot–Marie–Tooth types 1A and 1X, endoneurial fibroblasts also express CSF-1 and form similar cell–cell contacts with macrophages as in our genetic models, it is most likely that the cytokine plays a detrimental role in human Charcot–Marie–Tooth type 1. Therefore, CSF-1 or its cognate receptor are pivotal target candidates for future treatment approaches in human Charcot–Marie–Tooth disease.

Acknowledgements

The authors are grateful to Heinrich Blazyca, Silke Loserth, Hannelore Mader and Bettina Meyer for skilful technical assistance. Special thanks go to Helga Brünner and Karl-Heinz Aulenbach for sophisticated care of mice. We are grateful to Dr Carsten Wessig for electrophysiological recordings. The authors are most grateful to Prof. Claudia Sommer and Hiltrud Klüpfel for providing the biopsies from Patients X3 and NP, including corresponding clinical and genetic data. We would like to dedicate this article in honour of the outstanding and visionary neuroscientist, Professor John (Jack) W. Griffin, who sadly passed away in April 2011.

Funding

Our work was supported by the German Research Council (SFB581; A3, to R.M.; WE 1406/13-1 to J.W.); NIH grants (CA32551 and CA26504, to E.R.S.) and the Interdisciplinary

Centre for Clinical Research (IZKF, project A-122) of the University of Würzburg (to R.M.).

Supplementary material

Supplementary material is available at *Brain* online.

References

Abe R, Donnelly SC, Peng T, Bucala R, Metz CN. Peripheral blood fibrocytes: differentiation pathway and migration to wound sites. J Immunol 2001; 166: 7556–62.

Berciano J, Garcia A, Calleja J, Combarros O. Clinico-electrophysiological correlation of extensor digitorum brevis muscle atrophy in children with charcot-marie-tooth disease 1A duplication. Neuromuscular disorders: NMD 2000; 10: 419–24.

Burns J, Ouvrier RA, Yiu EM, Joseph PD, Kornberg AJ, Fahey MC, et al. Ascorbic acid for Charcot-Marie-Tooth disease type 1A in children: a randomised, double-blind, placebo-controlled, safety and efficacy trial. Lancet Neurol 2009; 8: 537–44.

Carenini S, Mäurer M, Werner A, Blazyca H, Toyka KV, Schmid CD, et al. The role of macrophages in demyelinating peripheral nervous system of mice heterozygously deficient in P0. J Cell Biol 2001; 152: 301–308.

Carvalho AA, Vital A, Ferrer X, Latour P, Lagueny A, Brechenmacher C, et al. Charcot-Marie-Tooth disease type 1A: clinicopathological correlations in 24 patients. J Peripher Nerv Syst 2005; 10: 85–92.

Chitu V, Stanley ER. Colony-stimulating factor-1 in immunity and inflammation. Curr Opin Immunol 2006; 18: 39–48.

Court FA, Gillingwater TH, Melrose S, Sherman DL, Greenshields KN, Morton AJ, et al. Identity, developmental restriction and reactivity of extralaminar cells capping mammalian neuromuscular junctions. J Cell Sci 2008; 121: 3901–11.

Crawford TO, Griffin JW. Morphometrical and ultrastructural evaluation of the sural nerve in children with Charcot-Marie-Tooth: implication for pathogenesis and treatment. Ann Neurol 1991; 30: 500.

D'Antonio M, Feltri ML, Wrabetz L. Myelin under stress. J Neurosci Res 2009; 87: 3241–9.

Dai XM, Zong XH, Sylvestre V, Stanley ER. Incomplete restoration of colony-stimulating factor 1 (CSF-1) function in CSF-1-deficient Csf1op/Csf1op mice by transgenic expression of cell surface CSF-1. Blood 2004; 103: 1114–23.

Fischer S, Kleinschnitz C, Müller M, Kobsar I, Ip CW, Rollins BJ, et al. Monocyte chemoattractant protein-1 is a pathogenic component in a model for a hereditary peripheral neuropathy. Mol Cell Neurosci 2008a; 37: 359–366.

Fischer S, Weishaupt A, Troppmair J, Martini R. Increase of MCP-1 (CCL2) in myelin mutant Schwann cells is mediated by MEK-ERK signaling pathway. Glia 2008b; 56: 836–43.

Gallardo E, Garcia A, Combarros O, Berciano J. Charcot-Marie-Tooth disease type 1A duplication: spectrum of clinical and magnetic resonance imaging features in leg and foot muscles. Brain 2006; 129: 426–37.

Grehl H, Schroder JM. Significance of degenerating endoneurial cells in peripheral neuropathy. Acta neuropathologica 1991; 81: 680–5.

Groh J, Heinl K, Kohl B, Wessig C, Greeske J, Fischer S, et al. Attenuation of MCP-1/CCL2 expression ameliorates neuropathy in a mouse model for Charcot-Marie-Tooth 1X. Hum Mol Genet 2010; 19: 3530–43.

Herzog EL, Bucala R. Fibrocytes in health and disease. Experimental Hematol 2010; 38: 548–56.

Hohlfeld R, Kerschensteiner M, Stadelmann C, Lassmann H, Wekerle H. The neuroprotective effect of inflammation: implications for the therapy of multiple sclerosis. J Neuroimmunol 2000; 107: 161–6.

Hristova M, Cuthill D, Zbarsky V, Acosta-Saltos A, Wallace A, Blight K, et al. Activation and deactivation of periventricular white matter phagocytes during postnatal mouse development. Glia 2010; 58: 11–28.

Huxley C, Passage E, Robertson AM, Youl B, Huston S, Manson A, et al. Correlation between varying levels and the degree of demyelination and reduction in nerve conduction velocity in transgenic mice. Hum Mol Genet 1998; 7: 449–58.

Ip CW, Kroner A, Bendszus M, Leder C, Kobsar I, Fischer S, et al. Immune cells contribute to myelin degeneration and axonopathic changes in mice overexpressing proteolipid protein in oligodendrocytes. J Neurosci 2006a; 26: 8206–16.

Ip CW, Kroner A, Fischer S, Berghoff M, Kobsar I, Mäurer M, et al. Role of immune cells in animal models for inherited peripheral neuropathies. Neuromol Med 2006b; 8: 175–89.

Joseph NM, Mukouyama YS, Mosher JT, Jaegle M, Crone SA, Dormand EL, et al. Neural crest stem cells undergo multilineage differentiation in developing peripheral nerves to generate endoneurial fibroblasts in addition to Schwann cells. Development 2004; 131: 5599–612.

Kalla R, Liu Z, Xu S, Koppius A, Imai Y, Kloss CU, et al. Microglia and the early phase of immune surveillance in the axotomized facial motor nucleus: impaired microglial activation and lymphocyte recruitment but no effect on neuronal survival or axonal regeneration in macrophage-colony stimulating factor-deficient mice. J Comp Neurol 2001; 436: 182–201.

Kerschensteiner M, Gallmeier E, Behrens L, Leal VV, Misgeld T, Klinkert WE, et al. Activated human T cells, B cells, and monocytes produce brain-derived neurotrophic factor in vitro and in inflammatory brain lesions: a neuroprotective role of inflammation? J Exp Med 1999; 189: 865–70.

Kobsar I, Berghoff M, Samsam M, Wessig C, Maurer M, Toyka KV, et al. Preserved myelin integrity and reduced axonopathy in connexin32-deficient mice lacking the recombination activating gene-1. Brain 2003; 126: 804–13.

Kohl B, Fischer S, Groh J, Wessig C, Martini R. MCP-1/CCL2 modifies axon properties in a PMP22-overexpressing mouse model for Charcot-Marie-Tooth 1A neuropathy. Am J Pathol 2010; 176: 1390–99.

Kondo Y, Adams JM, Vanier MT, Duncan ID. Macrophages counteract demyelination in a mouse model of globoid cell leukodystrophy. J Neurosci 2011; 31: 3610–24.

Linker RA, Lee DH, Demir S, Wiese S, Kruse N, Siglienti I, et al. Functional role of brain-derived neurotrophic factor in neuroprotective autoimmunity: therapeutic implications in a model of multiple sclerosis. Brain 2010; 133: 2248–63.

Martini R, Fischer S, Lopez-Vales R, David S. Interactions between Schwann cells and macrophages in injury and inherited demyelinating disease. Glia 2008; 56: 1566–77.

Mäurer M, Müller M, Kobsar I, Leonhard C, Martini R, Kiefer R. Origin of pathogenic macrophages and endoneurial fibroblast-like cells in an animal model of inherited neuropathy. Mol Cell Neurosci 2003; 23: 351–9.

Meyer zu Horste G, Prukop T, Liebetanz D, Mobius W, Nave KA, Sereda MW. Antiprogesterone therapy uncouples axonal loss from demyelination in a transgenic rat model of CMT1A neuropathy. Ann Neurol 2007; 61: 61–72.

Micallef J, Attarian S, Dubourg O, Gonnaud PM, Hogrel JY, Stojkovic T, et al. Effect of ascorbic acid in patients with Charcot-Marie-Tooth disease type 1A: a multicentre, randomised, double-blind, placebo-controlled trial. Lancet Neurol 2009; 8: 1103–10.

Muller M, Berghoff M, Kobsar I, Kiefer R, Martini R. Macrophage colony stimulating factor is a crucial factor for the intrinsic macrophage response in mice heterozygously deficient for the myelin protein P0. Exp Neurol 2007; 203: 55–62.

Nave KA. Myelination and support of axonal integrity by glia. Nature 2010; 468: 244–52.

Nelles E, Bützler C, Jung D, Temme A, Gabriel HD, Dahl U, et al. Defective propagation of signals generated by sympathetic nerve stimulation in the liver of connexin32-deficient mice. Proc Natl Acad Sci USA 1996; 93: 9565–70.

Niemann A, Berger P, Suter U. Pathomechanisms of mutant proteins in Charcot-Marie-Tooth disease. Neuromolecular Med 2006; 8: 217–42.

Ohara S, Takahashi H, Ikuta F. Specialised contacts of endoneurial fibroblasts with macrophages in wallerian degeneration. J Anatomy 1986; 148: 77–85.

Ohno H, Kubo K, Murooka H, Kobayashi Y, Nishitoba T, Shibuya M, et al. A c-fms tyrosine kinase inhibitor, Ki20227, suppresses osteoclast differentiation and osteolytic bone destruction in a bone metastasis model. Molecular Canc Therapeutics 2006; 5: 2634–43.

Ohno H, Uemura Y, Murooka H, Takanashi H, Tokieda T, Ohzeki Y, et al. The orally-active and selective c-Fms tyrosine kinase inhibitor Ki20227 inhibits disease progression in a collagen-induced arthritis mouse model. European J Immunol 2008; 38: 283–91.

Pareyson D, Reilly MM, Schenone A, Fabrizi GM, Cavallaro T, Santoro L, et al. Ascorbic acid in Charcot-Marie-Tooth disease type 1A (CMT-TRIAAL and CMT-TRAUK): a double-blind randomised trial. Lancet Neurol 2011; 10: 320–8.

Pareyson D, Solari A. Charcot-Marie-Tooth disease type 1A: is ascorbic acid effective? Lancet Neurol 2009; 8: 1075–1077.

Pennuto M, Tinelli E, Malaguti M, Del Carro U, D'Antonio M, Ron D, et al. Ablation of the UPR-Mediator CHOP restores motor function and reduces demyelination in Charcot-Marie-Tooth 1B Mice. Neuron 2008; 57: 393–405.

Peters A, Palay SL, Webster Hd. The fine structure of the nervous system. New York, Oxford: Oxford University Press; 1991.

Raivich G, Bohatschek M, Kloss CU, Werner A, Jones LL, Kreutzberg GW. Neuroglial activation repertoire in the injured brain: graded response, molecular mechanisms and cues to physiological function. Brain Res Brain Res Rev 1999; 30: 77–105.

Reilly MM, Murphy SM, Laura M. Charcot-Marie-Tooth disease. JPNS 2011; 16: 1–14.

Ryan GR, Dai XM, Dominguez MG, Tong W, Chuan F, Chisholm O, et al. Rescue of the colony-stimulating factor 1 (CSF-1)-nullizygous mouse (Csf1(op)/Csf1(op)) phenotype with a CSF-1 transgene and identification of sites of local CSF-1 synthesis. Blood 2001; 98: 74–84.

Schenone A, Nobbio L, Monti Bragadin M, Ursino G, Grandis M. Inherited neuropathies. Current treatment options in neurology 2011; 13: 160–79.

Scherer SS, Wrabetz L. Molecular mechanisms of inherited demyelinating neuropathies. Glia 2008; 56: 1578–89.

Schmidt B, Toyka KV, Kiefer R, Full J, Hartung HP, Pollard J. Inflammatory infiltrates in sural nerve biopsies in Guillain-Barre syndrome and chronic inflammatory demyelinating neuropathy. Muscle-Nerve 1996; 19: 474–87.

Schroder JM, Hoheneck M, Weis J, Deist H. Ethylene oxide polyneuropathy: clinical follow-up study with morphometric and electron microscopic findings in a sural nerve biopsy. J Neurol 1985; 232: 83–90.

Senderek J, Bergmann C, Quasthoff S, Ramaekers VT, Schröder JM. X-linked dominant Charcot-Marie-Tooth disease: nerve biopsies allow morphological evaluation and detection of connexin32 mutations (Arg15Trp, Arg22GIn). Acta Neuropathol 1998; 95: 443–49.

Senderek J, Hermanns B, Bergmann C, Boroojerdi B, Bajbouj M, Hungs M, et al. X-linked dominant Charcot-Marie-Tooth neuropathy: clinical, electrophysiological, and morphological phenotype in four families with different connexin32 mutations(1). J Neurological Sci 1999; 167: 90–101.

Stoll G, Gabreels-Festen AA, Jander S, Muller HW, Hanemann CO. Major histocompatibility complex class II expression and macrophage responses in genetically proven Charcot-Marie-Tooth type 1 and hereditary neuropathy with liability to pressure palsies. Muscle Nerve 1998; 21: 1419–27.

Teitelbaum SL. Bone resorption by osteoclasts. Science 2000; 289: 1504–8.

Thomas PK. The deposition of collagen in relation to Schwann cell basement membrane during peripheral nerve regeneration. J Cell Biol 1964; 23: 375–82.

Thomas PK. The cellular response to nerve injury. I. The cellular outgrowth from the distal stump of transected nerve. J Anat 1966; 1002: 287–303.

Trouvin AP, Goeb V. Receptor activator of nuclear factor-kappaB ligand and osteoprotegerin: maintaining the balance to prevent bone loss. Clinical Interv Aging 2010; 5: 345–54.

Uemura Y, Ohno H, Ohzeki Y, Takanashi H, Murooka H, Kubo K, et al. The selective M-CSF receptor tyrosine kinase inhibitor Ki20227 suppresses experimental autoimmune encephalomyelitis. J Neuroimmunol 2008; 195: 73–80.

Wei S, Nandi S, Chitu V, Yeung YG, Yu W, Huang M, et al. Functional overlap but differential expression of CSF-1 and IL-34 in their CSF-1 receptor-mediated regulation of myeloid cells. J Leukoc Biol 2010; 88: 495–505.

Yoshida H, Hayashi S-I, Kunisada T, Ogawa M, Nishikawa S, Okamura H, et al. The murine mutation osteopetrosis is in the coding region of the macrophage colony stimulating factor gene. Nature 1990; 345: 442–44.